Sciencexpress Reports

Commensal *Bifidobacterium* promotes antitumor immunity and facilitates anti–PD-L1 efficacy

Ayelet Sivan,[1]* Leticia Corrales,[1]* Nathaniel Hubert,[2] Jason B. Williams,[1] Keston Aquino-Michaels,[3] Zachary M. Earley,[2] Franco W. Benyamin,[1] Yuk Man Lei,[2] Bana Jabri,[2] Maria-Luisa Alegre,[2] Eugene B. Chang,[2] Thomas F. Gajewski[1,2]†

[1]Department of Pathology, University of Chicago, Chicago, IL, USA. [2]Department of Medicine, University of Chicago, Chicago, IL, USA. [3]Section of Genetic Medicine, University of Chicago, Chicago, IL, USA.

*These authors contributed equally to this work.

*Corresponding author. E-mail: tgajewsk@medicine.bsd.uchicago.edu

T cell infiltration of solid tumors is associated with favorable patient outcomes, yet the mechanisms underlying variable immune responses between individuals are not well understood. One possible modulator could be the intestinal microbiota. We compared melanoma growth in mice harboring distinct commensal microbiota and observed differences in spontaneous antitumor immunity, which were eliminated upon cohousing or following fecal transfer. 16*S* ribosomal RNA sequencing identified *Bifidobacterium* as associated with the antitumor effects. Oral administration of *Bifidobacterium* alone improved tumor control to the same degree as anti–PD-L1 therapy (checkpoint blockade), and combination treatment nearly abolished tumor outgrowth. Augmented dendritic cell function leading to enhanced CD8$^+$ T cell priming and accumulation in the tumor microenvironment mediated the effect. Our data suggest that manipulating the microbiota may modulate cancer immunotherapy.

Harnessing the host immune system constitutes a promising cancer therapeutic because of its potential to specifically target tumor cells while limiting harm to normal tissue. Enthusiasm has been fueled by recent clinical success, particularly with antibodies that block immune inhibitory pathways, specifically CTLA-4 and the PD-1/PD-L1 axis (*1*, *2*). Clinical responses to these immunotherapies are more frequent in patients who show evidence of an endogenous T cell response ongoing in the tumor microenvironment prior to therapy (*3*–*6*). However, the mechanisms that govern the presence or absence of this phenotype are not well understood. Theoretical sources of inter-patient heterogeneity include host germline genetic differences, variability in patterns of somatic alterations in tumor cells, and environmental differences.

The gut microbiota plays an important role in shaping systemic immune responses (*7*–*9*). In the cancer context, a role for intestinal microbiota in mediating immune activation in response to chemotherapeutic agents has been demonstrated (*10*, *11*). However, whether commensal microbiota influence spontaneous immune responses against tumors, thereby impacting therapeutic activity of immunotherapeutic interventions such as anti–PD-1/PD-L1 monoclonal antibodies, is unknown.

To address this question, we compared subcutaneous B16.SIY melanoma growth in genetically similar C57BL/6 mice derived from two different mouse facilities, Jackson Laboratory (JAX) and Taconic Farms (TAC), which have been shown to differ in their commensal microbes (*12*). We found that JAX and TAC mice exhibited significant differences in B16.SIY melanoma growth rate, with tumors growing more aggressively in TAC mice (Fig. 1A). This difference was immune-mediated: Tumor-specific T cell responses (Fig. 1, B and C) and intratumoral CD8$^+$ T cell accumulation (Fig. 1D) were significantly higher in JAX compared to TAC mice. To begin to address whether this difference could be mediated by commensal microbiota, we cohoused JAX and TAC mice prior to tumor implantation. We found that cohousing ablated the differences in tumor growth (Fig. 1E) and immune responses (Fig. 1, F to H) between the two mouse populations, arguing for an environmental influence. TAC mice appeared to acquire the JAX phenotype upon cohousing, suggesting that JAX mice may be colonized by commensal microbes that dominantly facilitate antitumor immunity.

To directly test the role of commensal bacteria in regulating antitumor immunity, we transferred JAX or TAC fecal suspensions into TAC and JAX recipients by oral gavage prior to tumor implantation (fig. S1A). We found that prophylactic transfer of JAX fecal material, but not saline or TAC fecal material, into TAC recipients was sufficient to delay tumor growth (Fig. 2A) and to enhance induction and infiltration of tumor-specific CD8$^+$ T cells (Fig. 2, B and C, and fig. S1B), supporting a microbe-derived effect. Reciprocal transfer of TAC fecal material into JAX recipients had a minimal effect on tumor growth rate and antitumor T cell responses (Fig. 2, A to C, and fig. S1B), consistent with the JAX-dominant effects observed upon cohousing.

To test whether manipulation of the microbial community could be effective as a therapy, we administered JAX fecal material alone or in combination with antibodies targeting PD-L1 (αPD-L1) to TAC mice bearing established tumors. Transfer of JAX fecal material alone resulted in significantly slower tumor growth (Fig. 2D), accompanied by increased tumor-specific T cell responses (Fig. 2E) and infiltration of antigen-specific T cells into the tumor (Fig. 2F), to the same degree as treatment with systemic αPD-L1 mAb. Combination treatment with both JAX fecal transfer and αPD-L1 mAb improved tumor control (Fig. 2D) and circulating tumor antigen-specific T cell responses (Fig. 2E), while there was little additive effect on accumulation of activated T cells within the tumor microenvironment (Fig. 2F). Consistent with these results, αPD-L1 therapy alone was significantly more efficacious in JAX mice compared to TAC mice (Fig. 2G), which paralleled improved antitumor T cell responses (fig. S1C). These data indicate that the commensal microbial composition can influence spontaneous antitumor immunity as well as response to immunotherapy with αPD-L1 mAb.

To identify specific bacteria associated with improved antitumor immune responses, we monitored the fecal bacterial content over time of mice that were subjected to administration of fecal permutations, using the 16*S* ribosomal RNA (rRNA) miSeq Illumina platform. Principal coordinate analysis revealed that fecal samples analyzed from TAC mice that received JAX fecal material gradually separated from samples obtained from sham- and TAC feces-inoculated TAC mice over time (P = 0.001 and P = 0.003, respectively, ANOSIM) and became similar to samples obtained from sham- and JAX feces-inoculated JAX mice (Fig. 3A). In contrast, TAC-inoculated TAC mice did not change in community diversity relative to sham-inoculated TAC mice (P = 0.4, ANOSIM). Reciprocal transfer of TAC fecal material into JAX hosts resulted in a statistically significant change in community diversity (P = 0.003, ANOSIM), yet the distance of the microbial shift was smaller (Fig. 3A).

Comparative analysis showed that 257 taxa were of significantly different relative abundance in JAX mice relative to TAC mice (FDR < 0.05, nonparametric *t*-test) (Fig. 3B and table S1). Members belonging to several of these groups were similarly altered in JAX-fed TAC mice relative to sham- or TAC-inoculated TAC mice (Fig. 3C and tables S1 and S2). To further identify functionally relevant bacterial taxa, we asked which genus-level taxa were significantly associated with accumulation of activated antigen-specific T cells within the tumor microenvironment across all permutations (Fig. 2C). The only significant association was *Bifidobacterium* ($P = 5.7 \times 10^{-5}$, FDR = 0.0019, univariate regression) (table S3), which showed a positive association with antitumor T cell responses and increased in relative abundance over 400-fold in JAX-fed TAC mice (Fig. 3C). Stimulatory interactions between bifidobacteria and the host immune system, including those associated with interferon (IFN)-γ, have been described previously (*13*–*16*). We thus hypothesized that members of this genus could represent a major component of the beneficial antitumor immune effects observed in JAX mice.

At the sequence level, *Bifidobacterium* operational taxonomic unit OTU_681370 showed the largest increase in relative abundance in JAX-fed TAC mice (table S1) and the strongest association with antitumor T cell responses across all permutations (Fig. 3D and table S3). We further identified this bacterium as most similar to *B. breve*, *B. longum* and *B. adolescentis* (99% identity). To test whether *Bifidobacterium* spp. may be sufficient to augment protective immunity against tumors, we obtained a commercially available cocktail of *Bifidobacterium* species, which included *B. breve* and *B. longum* and administered this by oral gavage, alone or in combination with αPD-L1, to TAC recipients bearing established tumors. Analysis of fecal bacterial content revealed that the most significant change in response to *Bifidobacterium* inoculation occurred in the *Bifidobacterium* genus (P = 0.0009, FDR = 0.015, nonparametric *t* test), with a 120-fold increase in OTU_681370 (fig. S2A and table S4), suggesting that the commercial inoculum contained bacteria that were at least 97% identical to the taxon identified in JAX and JAX-fed TAC mice. An increase in *Bifidobacterium* could also be detected by quantitative PCR (fig. S2B).

Bifidobacterium-treated mice displayed significantly improved tumor control in comparison to non-*Bifidobacterium* treated counterparts (Fig. 3E), which was accompanied by robust induction of tumor-specific T cells in the periphery (Fig. 3F) and increased accumulation of antigen-specific $CD8^+$ T cells within the tumor (Fig. 3G and fig. S2C). These effects were durable for several weeks (fig. S2, D and E).

The therapeutic effect of *Bifidobacterium* feeding was abrogated in CD8-depleted mice (fig. S3A), arguing that the mechanism was not direct but rather through host antitumor T cell responses. Heat inactivation of the bacteria prior to oral administration also abrogated the therapeutic effect on tumor growth and reduced tumor-specific T cell responses to baseline (fig. S3, B to D), suggesting that the antitumor effect requires live bacteria. As an alternative strategy, we tested the therapeutic effect of *B. breve* and *B. longum* strains obtained from the ATCC, which also showed significantly improved tumor control (fig. S4A). Administration of *Bifidobacterium* to TAC mice inoculated with B16 parental tumor cells or MB49 bladder cancer cells also resulted in delayed tumor outgrowth (fig. S4, B and C, respectively). Oral administration of *Lactobacillus murinus* to TAC mice, which was not among the overrepresented taxa in JAX-fed mice, had no effect on tumor growth (fig. S4D) or on tumor-specific T cell responses (fig. S4E), suggesting that modulation of antitumor immunity depends on the specific bacteria administered. Collectively, these data point to

Bifidobacterium as a positive regulator of antitumor immunity in vivo.

Upon inoculation with *Bifidobacterium*, a small set of species were altered in parallel with *Bifidobacterium* (ANOSIM, P = 0.003) (fig. S5A, table S4), however, they largely did not resemble the changes observed with JAX-feces administration. Although we observed reductions (~2- to 10-fold) in members of the order Clostridiales as well as in butyrate-producing species upon *Bifidobacterium* inoculation, which could point to an inhibitory effect on the regulatory T cell compartment (*17*–*19*), we did not observe any difference in the frequency of $CD4^+$ $Foxp3^+$ T cells in tumors isolated from JAX and TAC mice (fig. S5B). Thus, while we cannot definitively rule out an indirect effect, it is unlikely that *Bifidobacterium* is acting primarily through modulation of the abundance of other bacteria.

We next assessed whether translocation of *Bifidobacterium* was occurring into the mesenteric lymph nodes, spleen or tumor, however no *Bifidobacterium* was detected in any of the organs isolated from *Bifidobacterium*-gavaged tumor-bearing mice (fig. S5C). We thus concluded that the observed systemic immunological effects are likely occurring independently of bacterial translocation.

We subsequently interrogated the immunologic mechanisms underlying the observed differences in T cell responses between TAC, JAX, and *Bifidobacterium*-treated TAC mice (fig. S6A). $CD8^+$ SIY-specific 2C TCR Tg T cells exposed to tumors in JAX and *Bifidobacterium*-treated TAC mice exhibited greater expansion in the tumor-draining lymph node as compared to their counterparts in TAC mice (fig. S6B). However, they produced markedly greater IFN-γ in both the tumor draining lymph node and the spleen of JAX and *Bifidobacterium*-fed TAC tumor-bearing mice (Fig. 4A), consistent with our analyses of the endogenous T cell response (Figs. 1C, 2E, and 3F). These data pointed to an improvement in immune responses upstream of T cells, at the level of host dendritic cells (DCs). Consistent with this hypothesis, we found an increased percentage of major histocompatibility complex (MHC) Class II^{hi} DCs in the tumors of JAX and *Bifidobacterium*-treated TAC mice (Fig. 4B).

We therefore employed genome-wide transcriptional profiling of early tumor-infiltrating DCs isolated from TAC, JAX and *Bifidobacterium*-treated TAC mice (fig. S7A and table S5). Pathway analysis of 760 gene transcripts upregulated in both JAX and *Bifidobacterium*-treated TAC-derived DCs relative to DCs from untreated TAC mice identified cytokine-cytokine receptor interaction, T cell activation, and positive regulation of mononuclear cell proliferation as significantly enriched pathways (Fig. 4C and fig. S7B). Many of these genes have been shown to be critical for antitumor responses including those involved in $CD8^+$ T cell activation and costimulation [*H2-m2* (MHC-I), *Cd40*, *Cd70*, *Icam1*)] (*20*–*22*); DC maturation (*Relb, Ifngr2*) (*23*, *24*); antigen processing and cross presentation (*Tapbp*, *Rab27a*, *Slc11a1*) (*25*–*27*); chemokine-mediated recruitment of immune cells to the tumor microenvironment (*Cxcl9*, *Cx3cl1*, *Cxcr4*) (*28*–*30*); and type I interferon signaling (*Irf1*, *Ifnar2*, *Oas2*, *Ifi35*, *Ifitm1*) (*31*, *32*) (Fig. 4D and fig. S7C). Expression of these genes was also increased in murine bone marrow–derived DCs stimulated with *Bifidobacterium in vitro* (table S6), consistent with previous reports that these species of *Bifidobacterium* can directly elicit DC maturation and cytokine production (*13*).

To test whether functional differences in DCs isolated from TAC, JAX, and *Bifidobacterium*-treated TAC mice could be sufficient to explain the differences in T cell priming observed in vivo, we purified DCs from lymphoid tissues of naïve TAC, JAX, and *Bifidobacterium*-treated TAC mice and tested their ability to induce CFSE-labeled $CD8^+$ SIY-specific 2C TCR Tg T cell proliferation and acquisition of IFN-γ production in vitro. DCs purified from JAX and *Bifidobacterium*-treated TAC mice induced 2C T cell proliferation at lower antigen concentration compared to DCs purified from naïve TAC mice (fig. S8, A and B). Furthermore, at all antigen concentrations, JAX-derived DCs elicited elevated levels of T cell IFN-γ production (Fig. 4E and fig. S8A). We observed similar effects upon oral administration of *Bifidobacterium* to TAC mice prior to DC isolation (Fig. 4E and fig. S8A). Taken together, these data suggest that commensal *Bifidobacterium*-derived signals modulate the activation of DCs in the steady state, which in turn supports improved effector function of tumor-specific $CD8^+$ T cells.

Our studies demonstrate an unexpected role for commensal *Bifidobacterium* in enhancing antitumor immunity in vivo. Given that beneficial effects are observed in multiple tumor settings, and that alteration of innate immune function is observed, this improved antitumor immunity could be occurring in an antigen-independent fashion. The necessity for live bacteria may imply that *Bifidobacterium* colonizes a specific compartment within the gut that enables it to interact with host cells that are critical for modulating DC function, or to release soluble factors that disseminate systemically leading to improved DC function.

Our results do not rule out a contribution of other commensal bacteria species in having the capability to regulate antitumor immunity, either positively or negatively. Our data support the idea that one source of intersubject heterogeneity with regard to spontaneous antitumor immunity and therapeutic effects of antibodies targeting the PD-1/PD-L1 axis may be the composition of gut microbes, which could be manipulated for therapeutic benefit. These principles could apply to other immunotherapies such as antibodies targeting the CTLA-4 pathway. Similar analyses can be performed in humans using 16*S* rRNA sequencing of stool samples from patients receiving checkpoint blockade or

other immunotherapies, to identify commensals associated with clinical benefit.

REFERENCES AND NOTES

1. F. S. Hodi, S. J. O'Day, D. F. McDermott, R. W. Weber, J. A. Sosman, J. B. Haanen, R. Gonzalez, C. Robert, D. Schadendorf, J. C. Hassel, W. Akerley, A. J. van den Eertwegh, J. Lutzky, P. Lorigan, J. M. Vaubel, G. P. Linette, D. Hogg, C. H. Ottensmeier, C. Lebbé, C. Peschel, I. Quirt, J. I. Clark, J. D. Wolchok, J. S. Weber, J. Tian, M. J. Yellin, G. M. Nichol, A. Hoos, W. J. Urba, Improved survival with ipilimumab in patients with metastatic melanoma. *N. Engl. J. Med.* **363**, 711–723 (2010). Medline doi:10.1056/NEJMoa1003466
2. O. Hamid, C. Robert, A. Daud, F. S. Hodi, W. J. Hwu, R. Kefford, J. D. Wolchok, P. Hersey, R. W. Joseph, J. S. Weber, R. Dronca, T. C. Gangadhar, A. Patnaik, H. Zarour, A. M. Joshua, K. Gergich, J. Elassaiss-Schaap, A. Algazi, C. Mateus, P. Boasberg, P. C. Tumeh, B. Chmielowski, S. W. Ebbinghaus, X. N. Li, S. P. Kang, A. Ribas, Safety and tumor responses with lambrolizumab (anti-PD-1) in melanoma. *N. Engl. J. Med.* **369**, 134–144 (2013). Medline doi:10.1056/NEJMoa1305133
3. P. C. Tumeh, C. L. Harview, J. H. Yearley, I. P. Shintaku, E. J. Taylor, L. Robert, B. Chmielowski, M. Spasic, G. Henry, V. Ciobanu, A. N. West, M. Carmona, C. Kivork, E. Seja, G. Cherry, A. J. Gutierrez, T. R. Grogan, C. Mateus, G. Tomasic, J. A. Glaspy, R. O. Emerson, H. Robins, R. H. Pierce, D. A. Elashoff, C. Robert, A. Ribas, PD-1 blockade induces responses by inhibiting adaptive immune resistance. *Nature* **515**, 568–571 (2014). Medline doi:10.1038/nature13954
4. S. Spranger, R. M. Spaapen, Y. Zha, J. Williams, Y. Meng, T. T. Ha, T. F. Gajewski, Up-regulation of PD-L1, IDO, and T(regs) in the melanoma tumor microenvironment is driven by CD8(+) T cells. *Sci. Transl. Med.* **5**, 200ra116 (2013). Medline doi:10.1126/scitranslmed.3006504
5. R. R. Ji, S. D. Chasalow, L. Wang, O. Hamid, H. Schmidt, J. Cogswell, S. Alaparthy, D. Berman, M. Jure-Kunkel, N. O. Siemers, J. R. Jackson, V. Shahabi, An immune-active tumor microenvironment favors clinical response to ipilimumab. *Cancer Immunol. Immunother.* **61**, 1019–1031 (2012). Medline doi:10.1007/s00262-011-1172-6
6. T. F. Gajewski, J. Louahed, V. G. Brichard, Gene signature in melanoma associated with clinical activity: A potential clue to unlock cancer immunotherapy. *Cancer J.* **16**, 399–403 (2010). Medline doi:10.1097/PPO.0b013e3181eacbd8
7. L. V. Hooper, D. R. Littman, A. J. Macpherson, Interactions between the microbiota and the immune system. *Science* **336**, 1268–1273 (2012). Medline doi:10.1126/science.1223490
8. I. I. Ivanov II, K. Honda, Intestinal commensal microbes as immune modulators. *Cell Host Microbe* **12**, 496–508 (2012). Medline doi:10.1016/j.chom.2012.09.009
9. J. P. McAleer, J. K. Kolls, Maintaining poise: Commensal microbiota calibrate interferon responses. *Immunity* **37**, 10–12 (2012). Medline doi:10.1016/j.immuni.2012.07.001
10. N. Iida, A. Dzutsev, C. A. Stewart, L. Smith, N. Bouladoux, R. A. Weingarten, D. A. Molina, R. Salcedo, T. Back, S. Cramer, R. M. Dai, H. Kiu, M. Cardone, S. Naik, A. K. Patri, E. Wang, F. M. Marincola, K. M. Frank, Y. Belkaid, G. Trinchieri, R. S. Goldszmid, Commensal bacteria control cancer response to therapy by modulating the tumor microenvironment. *Science* **342**, 967–970 (2013). Medline doi:10.1126/science.1240527
11. S. Viaud, F. Saccheri, G. Mignot, T. Yamazaki, R. Daillère, D. Hannani, D. P. Enot, C. Pfirschke, C. Engblom, M. J. Pittet, A. Schlitzer, F. Ginhoux, L. Apetoh, E. Chachaty, P. L. Woerther, G. Eberl, M. Bérard, C. Ecobichon, D. Clermont, C. Bizet, V. Gaboriau-Routhiau, N. Cerf-Bensussan, P. Opolon, N. Yessaad, E. Vivier, B. Ryffel, C. O. Elson, J. Doré, G. Kroemer, P. Lepage, I. G. Boneca, F. Ghiringhelli, L. Zitvogel, The intestinal microbiota modulates the anticancer immune effects of cyclophosphamide. *Science* **342**, 971–976 (2013). Medline doi:10.1126/science.1240537
12. I. I. Ivanov II, K. Atarashi, N. Manel, E. L. Brodie, T. Shima, U. Karaoz, D. Wei, K. C. Goldfarb, C. A. Santee, S. V. Lynch, T. Tanoue, A. Imaoka, K. Itoh, K. Takeda, Y. Umesaki, K. Honda, D. R. Littman, Induction of intestinal Th17 cells by segmented filamentous bacteria. *Cell* **139**, 485–498 (2009). Medline doi:10.1016/j.cell.2009.09.033
13. P. López, M. Gueimonde, A. Margolles, A. Suárez, Distinct Bifidobacterium strains drive different immune responses in vitro. *Int. J. Food Microbiol.* **138**, 157–165 (2010). Medline doi:10.1016/j.ijfoodmicro.2009.12.023
14. O. Ménard, M.-J. Butel, V. Gaboriau-Routhiau, A.-J. Waligora-Dupriet, Gnotobiotic mouse immune response induced by *Bifidobacterium* sp. strains isolated from infants. *Appl. Environ. Microbiol.* **74**, 660–666 (2008). Medline doi:10.1128/AEM.01261-07
15. P. Dong, Y. Yang, W. P. Wang, The role of intestinal bifidobacteria on immune system development in young rats. *Early Hum. Dev.* **86**, 51–58 (2010). Medline doi:10.1016/j.earlhumdev.2010.01.002
16. T. Kawahara, T. Takahashi, K. Oishi, H. Tanaka, M. Masuda, S. Takahashi, M. Takano, T. Kawakami, K. Fukushima, H. Kanazawa, T. Suzuki, Consecutive oral administration of *Bifidobacterium longum* MM-2 improves the defense system against influenza virus infection by enhancing natural killer cell activity in a murine model. *Microbiol. Immunol.* **59**, 1–12 (2015). Medline doi:10.1111/1348-0421.12210
17. N. Arpaia, C. Campbell, X. Fan, S. Dikiy, J. van der Veeken, P. deRoos, H. Liu, J. R. Cross, K. Pfeffer, P. J. Coffer, A. Y. Rudensky, Metabolites produced by commensal bacteria promote peripheral regulatory T-cell generation. *Nature* **504**, 451–455 (2013). Medline doi:10.1038/nature12726
18. P. M. Smith, M. R. Howitt, N. Panikov, M. Michaud, C. A. Gallini, M. Bohlooly-Y, J. N. Glickman, W. S. Garrett, The microbial metabolites, short-chain fatty acids, regulate colonic Treg cell homeostasis. *Science* **341**, 569–573 (2013). Medline doi:10.1126/science.1241165
19. K. Atarashi, T. Tanoue, T. Shima, A. Imaoka, T. Kuwahara, Y. Momose, G. Cheng, S. Yamasaki, T. Saito, Y. Ohba, T. Taniguchi, K. Takeda, S. Hori, I. I. Ivanov II, Y. Umesaki, K. Itoh, K. Honda, Induction of colonic regulatory T cells by indigenous *Clostridium* species. *Science* **331**, 337–341 (2011). Medline doi:10.1126/science.1198469
20. M. F. Mackey, J. R. Gunn, C. Maliszewsky, H. Kikutani, R. J. Noelle, R. J. Barth Jr., Dendritic cells require maturation via CD40 to generate protective antitumor immunity. *J. Immunol.* **161**, 2094–2098 (1998). Medline
21. A. Scholer, S. Hugues, A. Boissonnas, L. Fetler, S. Amigorena, Intercellular adhesion molecule-1-dependent stable interactions between T cells and dendritic cells determine CD8+ T cell memory. *Immunity* **28**, 258–270 (2008). Medline doi:10.1016/j.immuni.2007.12.016
22. S. P. Bak, M. S. Barnkob, A. Bai, E. M. Higham, K. D. Wittrup, J. Chen, Differential requirement for CD70 and CD80/CD86 in dendritic cell-mediated activation of tumor-tolerized CD8 T cells. *J. Immunol.* **189**, 1708–1716 (2012). Medline doi:10.4049/jimmunol.1201271
23. J. Pan, M. Zhang, J. Wang, Q. Wang, D. Xia, W. Sun, L. Zhang, H. Yu, Y. Liu, X. Cao, Interferon-gamma is an autocrine mediator for dendritic cell maturation. *Immunol. Lett.* **94**, 141–151 (2004). Medline doi:10.1016/j.imlet.2004.05.003
24. A. R. Pettit, C. Quinn, K. P. MacDonald, L. L. Cavanagh, G. Thomas, W. Townsend, M. Handel, R. Thomas, Nuclear localization of RelB is associated with effective antigen-presenting cell function. *J. Immunol.* **159**, 3681–3691 (1997). Medline
25. E. B. Compeer, T. W. H. Flinsenberg, S. G. van der Grein, M. Boes, Antigen processing and remodeling of the endosomal pathway: Requirements for antigen cross-presentation. *Front. Immunol.* **3**, 37 (2012). Medline doi:10.3389/fimmu.2012.00037
26. C. Jancic, A. Savina, C. Wasmeier, T. Tolmachova, J. El-Benna, P. M. Dang, S. Pascolo, M. A. Gougerot-Pocidalo, G. Raposo, M. C. Seabra, S. Amigorena, Rab27a regulates phagosomal pH and NADPH oxidase recruitment to dendritic cell phagosomes. *Nat. Cell Biol.* **9**, 367–378 (2007). Medline doi:10.1038/ncb1552
27. C. B. Stober, S. Brode, J. K. White, J. F. Popoff, J. M. Blackwell, Slc11a1, formerly Nramp1, is expressed in dendritic cells and influences major histocompatibility complex class II expression and antigen-presenting cell function. *Infect. Immun.* **75**, 5059–5067 (2007). Medline doi:10.1128/IAI.00153-07
28. K. Kabashima, N. Shiraishi, K. Sugita, T. Mori, A. Onoue, M. Kobayashi, J. Sakabe, R. Yoshiki, H. Tamamura, N. Fujii, K. Inaba, Y. Tokura, CXCL12-CXCR4 engagement is required for migration of cutaneous dendritic cells. *Am. J. Pathol.* **171**, 1249–1257 (2007). Medline doi:10.2353/ajpath.2007.070225
29. M. Nukiwa, S. Andarini, J. Zaini, H. Xin, M. Kanehira, T. Suzuki, T. Fukuhara, H. Mizuguchi, T. Hayakawa, Y. Saijo, T. Nukiwa, T. Kikuchi, Dendritic cells modified to express fractalkine/CX3CL1 in the treatment of preexisting tumors. *Eur. J. Immunol.* **36**, 1019–1027 (2006). Medline doi:10.1002/eji.200535549
30. L. Zhang, J. R. Conejo-Garcia, D. Katsaros, P. A. Gimotty, M. Massobrio, G. Regnani, A. Makrigiannakis, H. Gray, K. Schlienger, M. N. Liebman, S. C. Rubin, G. Coukos, Intratumoral T cells, recurrence, and survival in epithelial ovarian cancer. *N. Engl. J. Med.* **348**, 203–213 (2003). Medline doi:10.1056/NEJMoa020177
31. M. B. Fuertes, A. K. Kacha, J. Kline, S. R. Woo, D. M. Kranz, K. M. Murphy, T. F.

Gajewski, Host type I IFN signals are required for antitumor CD8+ T cell responses through CD8alpha+ dendritic cells. *J. Exp. Med.* **208**, 2005–2016 (2011). Medline doi:10.1084/jem.20101159
32. S.-R. Woo, M. B. Fuertes, L. Corrales, S. Spranger, M. J. Furdyna, M. Y. Leung, R. Duggan, Y. Wang, G. N. Barber, K. A. Fitzgerald, M. L. Alegre, T. F. Gajewski, STING-dependent cytosolic DNA sensing mediates innate immune recognition of immunogenic tumors. *Immunity* **41**, 830–842 (2014). Medline doi:10.1016/j.immuni.2014.10.017
33. C. Blank, I. Brown, A. C. Peterson, M. Spiotto, Y. Iwai, T. Honjo, T. F. Gajewski, PD-L1/B7H-1 inhibits the effector phase of tumor rejection by T cell receptor (TCR) transgenic CD8+ T cells. *Cancer Res.* **64**, 1140–1145 (2004). Medline doi:10.1158/0008-5472.CAN-03-3259
34. J. G. Caporaso, J. Kuczynski, J. Stombaugh, K. Bittinger, F. D. Bushman, E. K. Costello, N. Fierer, A. G. Peña, J. K. Goodrich, J. I. Gordon, G. A. Huttley, S. T. Kelley, D. Knights, J. E. Koenig, R. E. Ley, C. A. Lozupone, D. McDonald, B. D. Muegge, M. Pirrung, J. Reeder, J. R. Sevinsky, P. J. Turnbaugh, W. A. Walters, J. Widmann, T. Yatsunenko, J. Zaneveld, R. Knight, QIIME allows analysis of high-throughput community sequencing data. *Nat. Methods* **7**, 335–336 (2010). Medline doi:10.1038/nmeth.f.303
35. D. McDonald, M. N. Price, J. Goodrich, E. P. Nawrocki, T. Z. DeSantis, A. Probst, G. L. Andersen, R. Knight, P. Hugenholtz, An improved Greengenes taxonomy with explicit ranks for ecological and evolutionary analyses of bacteria and archaea. *ISME J.* **6**, 610–618 (2012). Medline doi:10.1038/ismej.2011.139
36. J. G. Caporaso, K. Bittinger, F. D. Bushman, T. Z. DeSantis, G. L. Andersen, R. Knight, PyNAST: A flexible tool for aligning sequences to a template alignment. *Bioinformatics* **26**, 266–267 (2010). Medline doi:10.1093/bioinformatics/btp636
37. Q. Wang, G. M. Garrity, J. M. Tiedje, J. R. Cole, Naive Bayesian classifier for rapid assignment of rRNA sequences into the new bacterial taxonomy. *Appl. Environ. Microbiol.* **73**, 5261–5267 (2007). Medline doi:10.1128/AEM.00062-07
38. C. Lozupone, R. Knight, UniFrac: A new phylogenetic method for comparing microbial communities. *Appl. Environ. Microbiol.* **71**, 8228–8235 (2005). Medline doi:10.1128/AEM.71.12.8228-8235.2005
39. I. Letunic, P. Bork, Interactive Tree Of Life v2: Online annotation and display of phylogenetic trees made easy. *Nucleic Acids Res.* **39** (suppl.), W475–W478 (2011). Medline doi:10.1093/nar/gkr201
40. M. Barman, D. Unold, K. Shifley, E. Amir, K. Hung, N. Bos, N. Salzman, Enteric salmonellosis disrupts the microbial ecology of the murine gastrointestinal tract. *Infect. Immun.* **76**, 907–915 (2008). Medline doi:10.1128/IAI.01432-07
41. Z. M. Earley, S. Akhtar, S. J. Green, A. Naqib, O. Khan, A. R. Cannon, A. M. Hammer, N. L. Morris, X. Li, J. M. Eberhardt, R. L. Gamelli, R. H. Kennedy, M. A. Choudhry, Burn injury alters the intestinal microbiome and increases gut permeability and bacterial translocation. *PLOS ONE* **10**, e0129996 (2015). 10.1371/journal.pone.0129996 Medline doi:10.1371/journal.pone.0129996
42. J.-P. Furet, O. Firmesse, M. Gourmelon, C. Bridonneau, J. Tap, S. Mondot, J. Doré, G. Corthier, Comparative assessment of human and farm animal faecal microbiota using real-time quantitative PCR. *FEMS Microbiol. Ecol.* **68**, 351–362 (2009). Medline doi:10.1111/j.1574-6941.2009.00671.x

ACKNOWLEDGMENTS

R code for gene expression analyses can be found at https://github.com/kipkeston/TG_Microbiota; microarray data can be found at http://www.ncbi.nlm.nih.gov/geo/query/acc.cgi?acc=GSE73475 and http://www.ncbi.nlm.nih.gov/geo/query/acc.cgi?acc=GSE73476; 16*S* rRNA sequencing data can be found at http://www.ncbi.nlm.nih.gov/bioproject/297465. The data reported in this manuscript are presented in the main paper and in the supplementary materials. We would like to thank D. Ringus for anaerobic culture of bifidobacteria and colony quantification, Y. Zhang for providing *Lactobacillus murinus* cultures, and R. Sweis for providing the MB49 bladder cancer cell line. This work was supported by a Team Science Award from the Melanoma Research Alliance, an National Institute of Diabetes and Digestive and Kidney Diseases, NIH, P30 Digestive Disease Research Core Center Grant (DK42086), the University of Chicago Cancer Biology training program (5T32CA009594-25), and the Cancer Research Institute fellowship program. The University of Chicago has filed a patent application that relates to microbial community manipulation in cancer therapy.

SUPPLEMENTARY MATERIALS

www.sciencemag.org/cgi/content/full/science.aac4255/DC1
Materials and Methods
Figs. S1 to S8
Tables S1 to S7
References (*33*–*42*)

25 April 2015; accepted 09 October 2015
Published online 5 November 2015
10.1126/science.aac4255

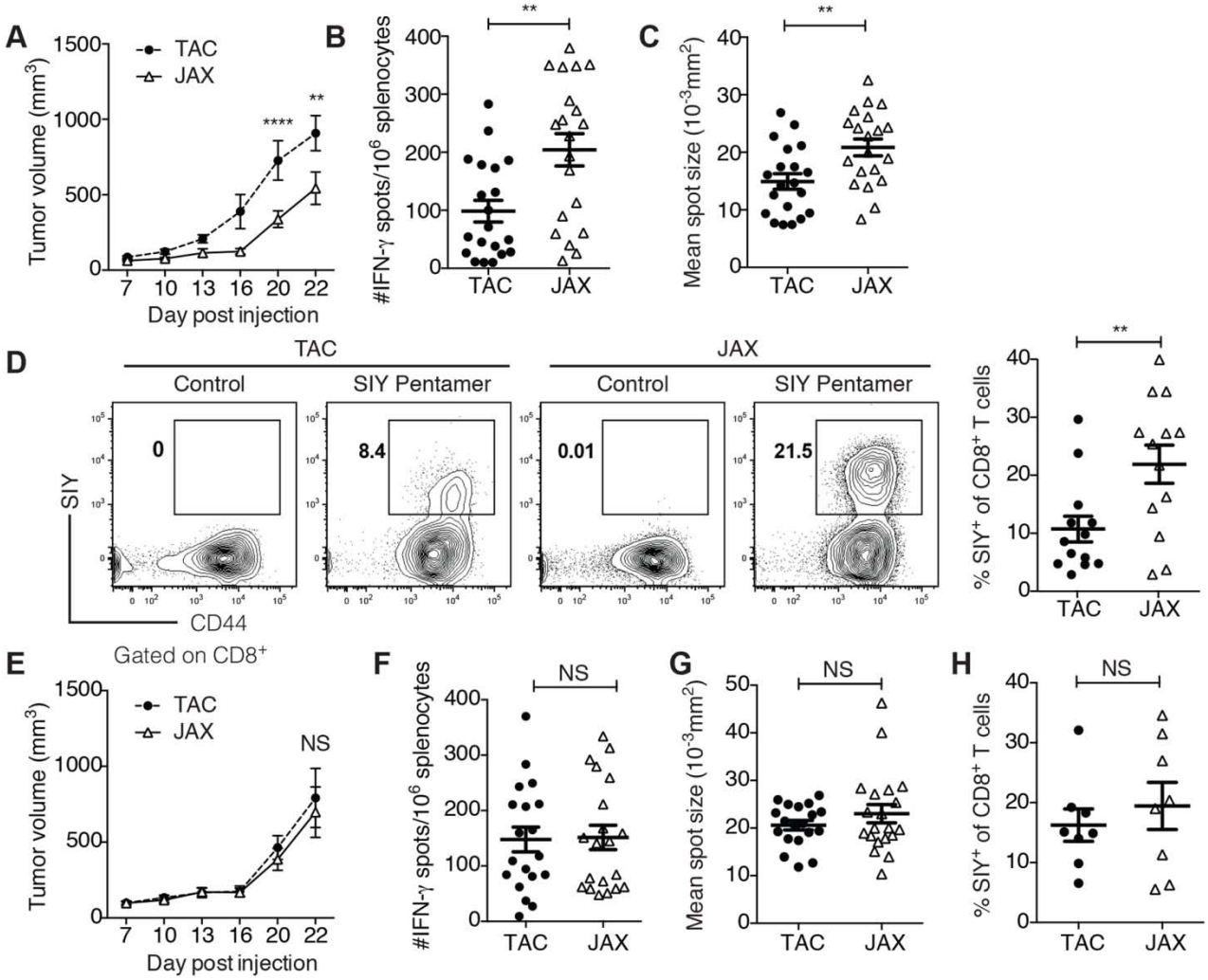

Fig. 1. Differences in melanoma outgrowth and tumor-specific immune responses between C57BL/6 JAX and TAC mice are eliminated upon cohousing. (**A**) B16.SIY tumor growth kinetics in newly arrived JAX and TAC mice. (**B**) IFN-γ ELISPOT in tumor-bearing JAX and TAC mice 7 days following tumor inoculation. (**C**) Mean size of IFN-γ spots (10^{-3} mm^2). (**D**) Percentage of SIY^+ T cells of total $CD8^+$ T cells within the tumor of JAX and TAC mice as determined by flow cytometry 21 days post-tumor inoculation. Representative plots (left), quantification (right). (**E**) B16.SIY tumor growth kinetics in JAX and TAC mice cohoused for 3 weeks prior to tumor inoculation. (**F**) Number of IFN-γ spots/10^6 splenocytes in tumor-bearing JAX and TAC mice cohoused for 3 weeks prior to tumor inoculation. (**G**) Mean size of IFN-γ spots (10^{-3} mm^2). (**H**) Percentage of SIY^+ T cells of total $CD8^+$ T cells within the tumor of JAX and TAC mice cohoused for 3 weeks prior to tumor inoculation. Data show mean ± SEM combined from six independent experiments, analyzed by two-way analysis of variance (ANOVA) with Sidak's correction for multiple comparisons [(A) and (E)], or individual mice with mean ± SEM combined from four [(B), (C), (F), (G)] or three [(D) and (H)] independent experiments, analyzed by Student's *t* test; 5 mice per group per experiment; $^{**}P < 0.01$, $^{****}P < 0.0001$, NS, not significant.

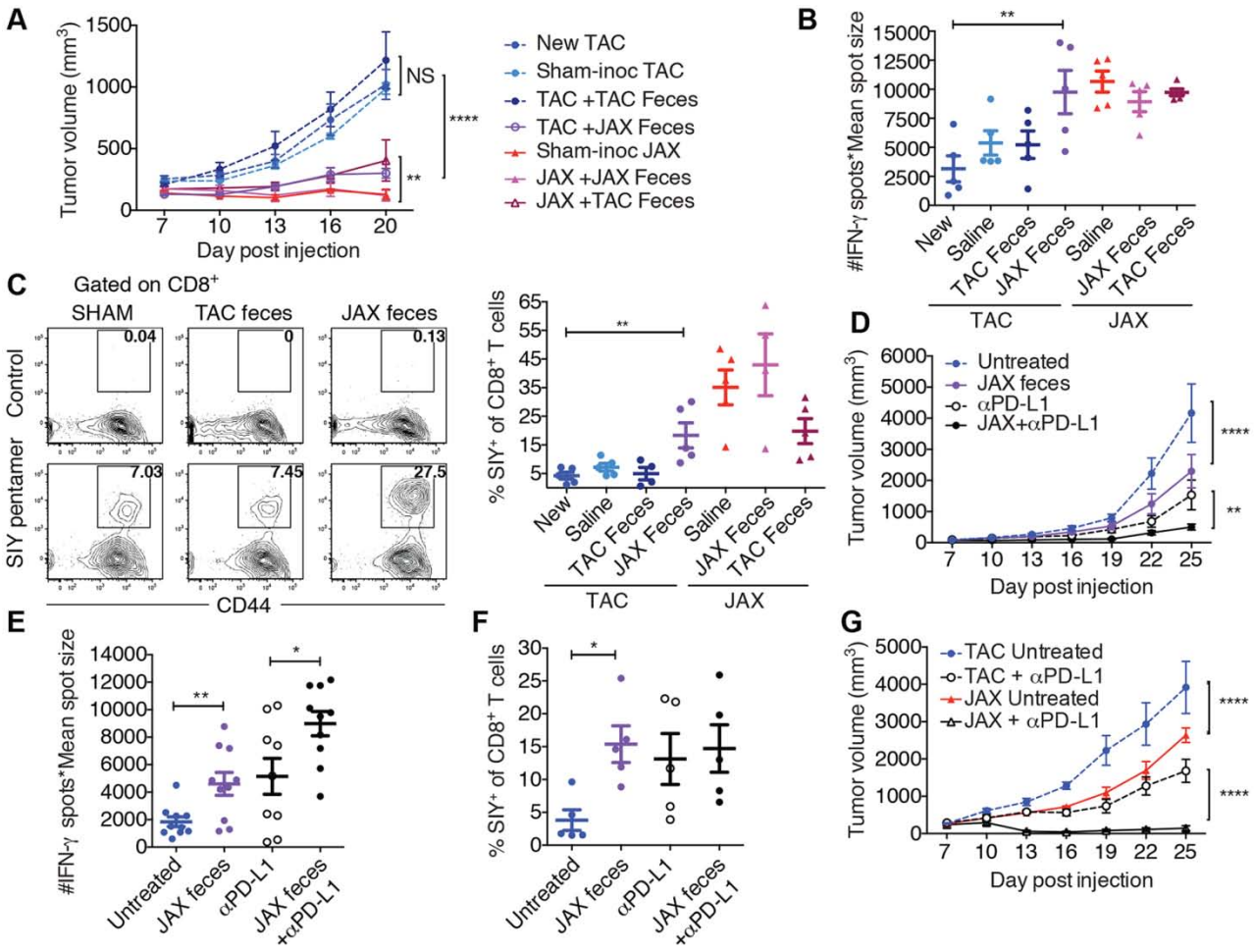

Fig. 2. Oral administration of JAX fecal material to TAC mice enhances spontaneous antitumor immunity and response to αPD-L1 mAb therapy. (**A**) B16.SIY tumor growth in newly arrived TAC mice, TAC and JAX mice orally gavaged with PBS, TAC or JAX fecal material prior to tumor implantation. (**B**) Number of IFN-γ spots × mean spot size (10^{-3} mm^2), determined by ELISPOT 7 days following tumor inoculation. (**C**) Percentage of SIY^+ $CD8^+$ T cells within the tumor of TAC and JAX mice treated as in (A), 21 days post-tumor inoculation. Representative plots (left), quantification (right). (**D**) B16.SIY tumor growth in TAC mice, untreated or treated with JAX fecal material 7 and 14 days post tumor implantation, αPD-L1 mAb 7, 10, 13 and 16 days post tumor implantation, or both regimens. (**E**) IFN-γ ELISPOT assessed 5 days after start of treatment. (**F**) Percentage of tumor-infiltrating SIY^+ $CD8^+$ T cells, determined by flow cytometry 14 days after start of treatment. (**G**) B16.SIY tumor growth kinetics in TAC and JAX mice, untreated or treated with αPD-L1 mAb 7, 10, 13 and 16 days post tumor implantation. Data show means ± SEM analyzed by two-way ANOVA with Dunnett's (A) or Tukey's [(D) and (G)] correction for multiple comparisons; or individual mice with means ± SEM analyzed by one-way ANOVA with Holm-Sidak correction for multiple comparisons [(B), (C), (E), (F)]; data are representative of [(A) to (C), (F), and (G)] or combined from [(D) and (E)] two to four independent experiments; 5 mice per group per experiment; $*P < 0.05$, $**P < 0.01$, $****P < 0.0001$, NS, not significant.

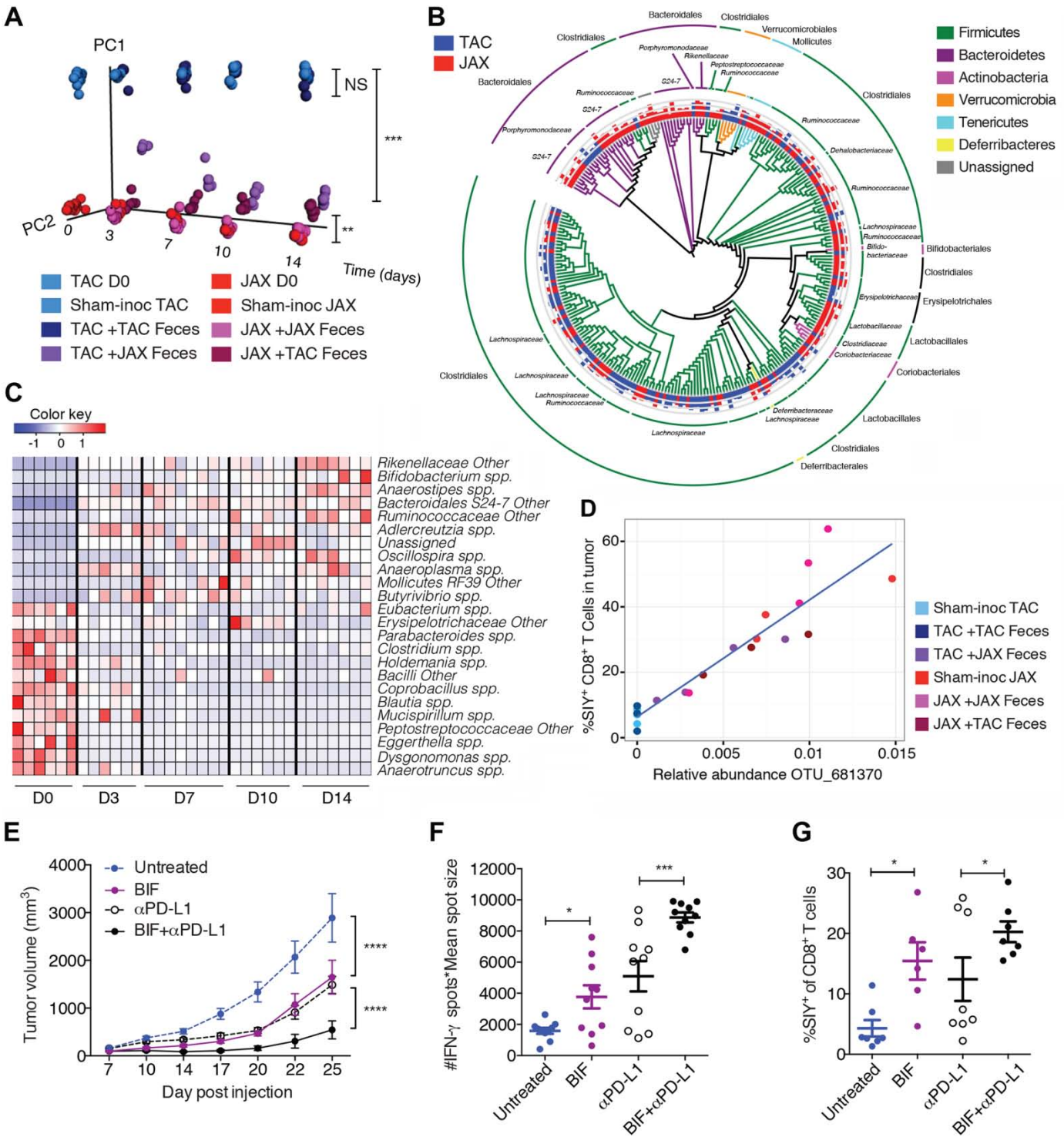

Fig. 3. Direct administration of *Bifidobacterium* to TAC recipients with established tumors improves tumor-specific immunity and response to αPD-L1 mAb therapy. (**A**) Principal coordinate analysis plot of bacterial β-diversity over time in groups treated as in Fig. 2A, each group is comprised of at least two cages, 3-4 mice per cage; data represent three independent experiments; $^{**}P < 0.01$, $^{***}P < 0.001$

Fig. 3. (cont.) (ANOSIM). (**B**) Phylogenetic analysis of taxa that are of significantly different abundance in newly arrived JAX vs TAC mice FDR<0.05 (nonparametric *t* test); bars represent log-transformed fold changes, inner circle = $\log_{10}(10)$; middle circle = $\log_{10}(100)$; outer circle = $\log_{10}(1000)$. (**C**) Heatmap demonstrating relative abundance over time of significantly altered genus-level taxa in JAX-fed TAC mice FDR<0.05 (nonparametric *t* test); columns depict individual mice; each timepoint shows mice from two separate cages, 3-4 mice per cage. (**D**) Correlation plot of relative abundance of *Bifidobacterium* OTU_681370 in fecal material obtained from groups as in (A) 14 days post arrival and frequency of SIY^+ $CD8^+$ T cells in tumor; $P = 1.4 \times 10^{-5}$, FDR = 0.0002, $R^2 = 0.86$ (univariate regression). (**E**) B16.SIY tumor growth kinetics in TAC mice, untreated or treated with *Bifidobacterium* 7 and 14 days post tumor implantation, αPD-L1 mAb 7, 10, 13 and 16 days post tumor implantation, or both regimens. (**F**) IFN-γ ELISPOT assessed 5 days after start of treatment. (**G**) Percentage of tumor-infiltrating SIY^+ $CD8^+$ T cells, determined by flow cytometry 14 days following start of treatment. Data show means ± SEM analyzed by two-way ANOVA with Tukey's correction (E) or individual mice with means ± SEM analyzed by one-way ANOVA with Holm-Sidak correction [(F) and (G)], and are combined from two independent experiments; 5 mice per group per experiment, $*P < 0.05$, $***P < 0.001$ $****P < 0.0001$.

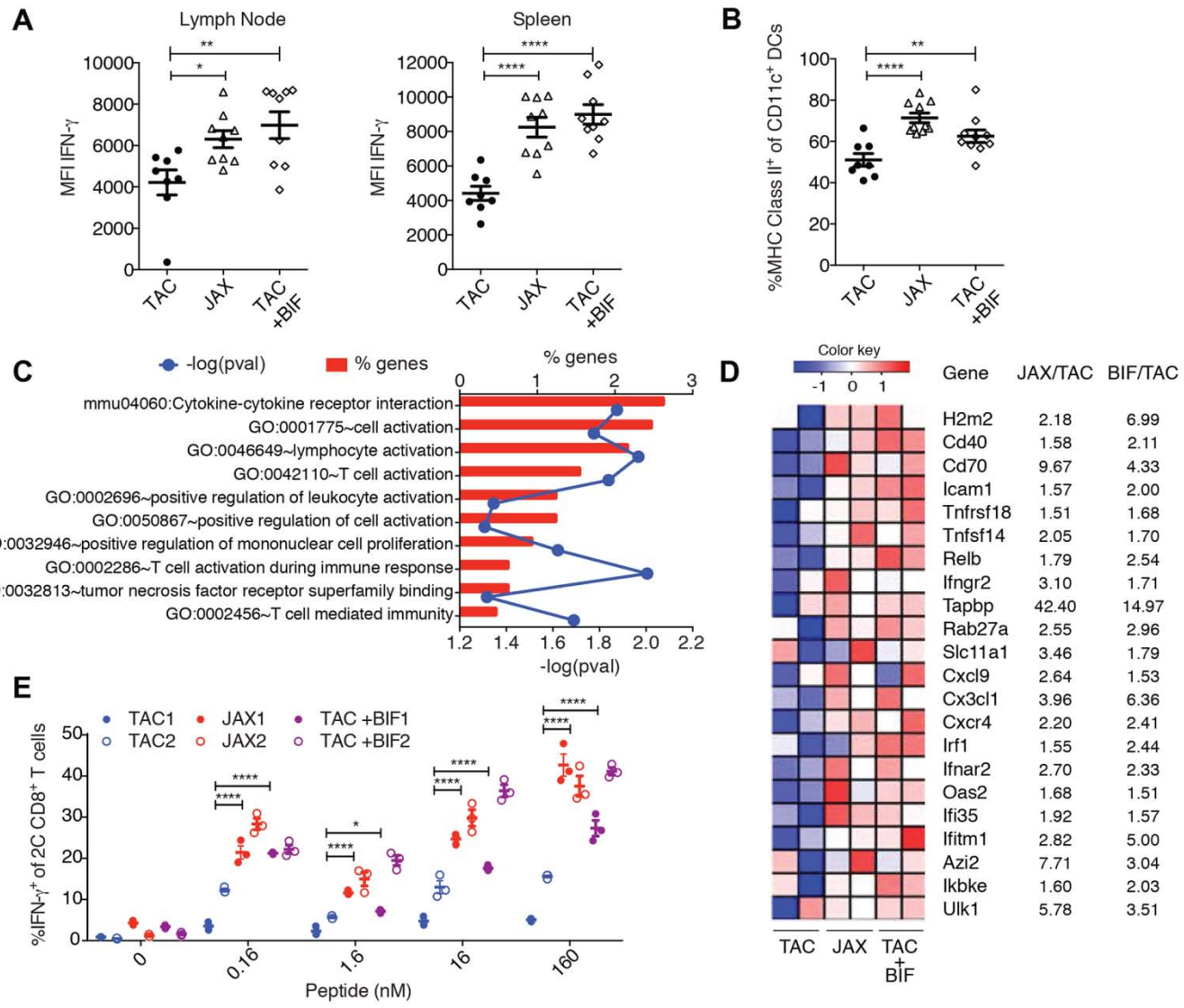

Fig. 4. Dendritic cells isolated from JAX and *Bifidobacterium*-fed TAC mice show increased expression of genes associated with antitumor immunity and heightened capability for T cell activation. (**A**) Quantification of IFN-γ MFI (mean fluorescence intensity) of 2C CD8$^+$ T cells in the tumor-draining lymph node (left) and spleen (right) of TAC, JAX, *Bifidobacterium*-fed TAC mice on day 7 post adoptive transfer. (**B**) Percentage of MHC Class II^{hi} DCs in tumors isolated from TAC, JAX, and *Bifidobacterium*-fed TAC mice 40 hours post tumor implantation as assessed by flow cytometry. Data in [(A) and (B)] show individual mice with mean ± SEM, analyzed by one-way ANOVA with Holm-Sidak correction; representative of two to four independent experiments, 8-9 mice per group per experiment, *P < 0.05, **P < 0.01, ****P < 0.0001. (**C**) Enriched biological pathways and functions found within the subset of elevated genes in JAX and *Bifidobacterium*-treated TAC-derived DCs relative to untreated TAC DCs isolated from tumors 40hrs post tumor inoculation, as assessed by DAVID pathway analysis. Red bars indicate the percent of genes in a pathway upregulated in DCs isolated from JAX and *Bifidobacterium*-fed TAC mice. Blue line indicates P values calculated by Fisher's exact test. (**D**) Heat map of key antitumor immunity genes in DCs isolated from JAX, *Bifidobacterium*-treated TAC or untreated TAC mice. Mean fold-change for each gene transcript is shown on the right. (**E**) Quantification of IFN-γ$^+$ 2C TCR Tg CD8$^+$ T cells stimulated in vitro with DCs purified from peripheral lymphoid tissues of naive TAC, JAX, and *Bifidobacterium*-treated TAC mice in the presence of different concentrations of SIY peptide. Analyses in [(C) to (E)] were performed on data combined from two independent experiments, 5 mice pooled per group per experiment. Data in [(E)] show technical replicates of pooled samples from each experiment separately, and were analyzed by fitting a linear mixed model, with Bonferroni correction for multiple comparisons; *P < 0.05, ****P < 0.0001.